Functionalization of SiC-based materials by a selective $YBa_2Cu_3O_{7-\delta}$ coating via sol–gel route in order to optimize their optical properties

Jessica Mollicone [a], Pascal Lenormand [a], Florence Ansart [a], Benoît Rousseau [b]

[a] CIRIMAT, Inter-University Material Research and Engineering Centre, Toulouse University, 118 Route de Narbonne 31062 Toulouse cedex 9, France
[b] LTN-UMR CNRS 6607, rue Christian Pauc, 44302 Nantes cedex 3, France

Keywords:
Functionalization
SiC
Sol–gel
Coating
Spectral selectivity

A B S T R A C T

SiC-based materials are good candidates for the application as solar receivers except concerning their optical properties. Indeed, considering the use at high temperature, materials used as solar receivers have to efficiently absorb the visible-near infrared waves (corresponding to solar spectral range) and simultaneously reflect the mid and far-infrared rays but SiC is absorbent in all the whole visible-infrared spectral domain. In this challenging work, a suitable $YBa_2Cu_3O_{7-\delta}$ oxide which can present appropriate optical properties is studied. It was synthesized following a sol–gel route and it was obtained with a high level of purity. $YBa_2Cu_3O_{7-\delta}$ pellets were realized and heat treated at different temperatures revealing that the higher the heat treatment is, the better the oxygen stoichiometry (7-δ) is and the smoothest the surface is. This directly acts on the $YBa_2Cu_3O_{7-\delta}$ optical properties. Considering these results, an $YBa_2Cu_3O_{7-\delta}$ coating was realized on SiC pellets by dip-coating. A homogenous and covering layer of about 10 μm was obtained presenting very promising optical properties which were predominant in the FIR-MIR range whereas absorptance was increased in NIR-visible range.

1. Introduction

Solar thermal energy processes are able to play an important role in providing both thermal energy and electrical energy for use in industry and in the residential sector. Among the different technologies, concentrated solar power plants appear promising for the conversion of solar radiation in hot air which drives a heat engine connected to an electrical power generator.

Between all the optical systems used to collect the incoming solar radiation, the solar receiver that must deliver hot air is one of the key components. To design it, porous ceramic foams appear very interesting in the range of 300–1200 °C because of their large specific surface which directly heats the air flowing through them. Generally, porous SiC-based materials are chosen as solar receivers because of their high temperature mechanical resistance [1]. Note that materials used as solar receivers have to efficiently absorb the visible-near infrared waves (corresponding to the solar spectral range). Simultaneously it has to reflect the mid and far-infrared rays (responsible for the thermal losses) and thus it has to present a low emittance in this spectral domain. This rule defines here the spectral selectivity. However, selected SiC compounds absorb all rays in the whole visible-infrared spectral domain making them less optimized for our purpose [2]. In order to enhance the spectral selectivity of volumetric absorbers, several works consisting of bilayer structures have been studied. [3] presents a two-slab structure: the first slab is composed of glass-beads transmitting the solar rays to the absorbent second slab made of silica honeycomb. Another way to make bilayer structure is to functionalize the absorber with a selective coating: [4], [5] or [6] present different spinel oxide coatings with a high temperature and oxidation stability and good selective efficiencies, showing that oxide coatings can be a suitable way to improve spectral selectivity of SiC absorbers.

To solve this challenging issue, a first step is to enhance the spectral selectivity of SiC receivers by depositing a suitable coating with appropriate optical properties on the whole solid network. $YBa_2Cu_3O_{7-\delta}$ coatings, when their thicknesses are higher than 400 nm and for $\delta \sim 0.2$–0.1, present a high reflectance in the mid-infrared spectral range and a high absorptance in the near infrared and visible spectral range at T = 20 °C [7] [8]. The understanding of the required experimental conditions to elaborate efficient $YBa_2Cu_3O_{7-\delta}$ coatings on 2D planar substrates will be used to foresee the passage towards the coating of 3D open-cell foams. To obtain the $YBa_2Cu_3O_{7-\delta}$ oxide, a lot of routes are available. It is thus possible to synthesize $YBa_2Cu_3O_{7-\delta}$ starting with metal acetate precursors, water, acetic acid and tri-ethanolamine followed by an adapted thermal treatment [9]. It is also possible to use metal alkoxides as starting materials but this route needs a lot of different solvents to dissolve the precursors [10]. These routes allow the coating of substrates by dip-coating but need several dips to obtain a thick layer. A different way to realize a thicker coating is by using vacuum coevaporation of Y, Cu and BaF_2 on the substrate [11] but this technique creates hydrofluoric acid vapor and is difficult to use on complex substrates as foams. We propose here a versatile way to synthesize the $YBa_2Cu_3O_{7-\delta}$

E-mail address: mollicone@chimie.ups-tlse.fr (J. Mollicone).

oxide by sol–gel route based on the Pechini's patent [12] allowing to easily control both the stoichiometry and the nanostructure of the synthesized oxide. Then, the crystallized powder obtained after a suitable thermal treatment is dispersed into an azeotropic solvent allowing to shape, after dipping the substrate into the suspension, a thick $YBa_2Cu_3O_{7-\delta}$ layer of about 10 μm.

However, the spectral selectivity of $YBa_2Cu_3O_{7-\delta}$ depends on the oxygen stoichiometry, which is governed by the thermal treatment used to synthesize it [13]. Many experimental methods have been used to evaluate the oxygen content in the $YBa_2Cu_3O_{7-\delta}$ samples: iodometric titration [14], thermogravimetric analysis [15], but all these measurements are destructive. [16] implemented a method to calculate oxygen stoichiometry based on the crystallographic cell parameters and the orthorhombicity degree. This non-destructive method seems to be the most suitable for this study. In this work, $YBa_2Cu_3O_{7-\delta}$ oxide is firstly synthesized and then SiC pellets with an $YBa_2Cu_3O_{7-\delta}$-type coating are studied, in particular its optical properties. The influence of the oxygen stoichiometry and the microstructure on the optical properties at room temperature are then evidenced.

2. Experimental

2.1. Materials

SiC pellets are first used as substrates, SiC powder synthesized by SICAT Company (Willstätt, Germany) is mixed with a binder (a solution of Rhodoviol 4/125, Prolabo) and pressed in a pelletizer with a pressure of 15 t. SiC pellets are sintered at 700 °C during 2 h with a heating rate of 100 °C/h which leads to pellets with a diameter of 20 mm and a thickness of 2 mm.

A route derived from the Pechini's patent [12] is used to prepare a precursor sol which leads to the formation of a metallic oxide ($YBa_2Cu_3O_{7-\delta}$ in this study) after a suitable heat treatment that we will discuss later. This process, followed by a suitable heat treatment, allows easily synthesizing various oxides with a totally controlled stoichiometry.

Two kinds of starting materials are used: inorganic compounds (metallic nitrates) providing cations and organic compounds such as acetylacetone (acac, Sigma-Aldrich 99%, chelating agent) and hexamethylenetetraamine (HMTA, Sigma-Aldrich 99%, polymeric precursor). A polymeric chain is formed by a hydrolysis reaction between HMTA and acac organic compounds. The cations are then homogeneously distributed through a complexation process in the structural network. The precursor sol is so prepared using acetic acid and water as solvents.

The nitrates $Y(NO_3)_3$, $6H_2O$ (Aldrich, 99.9%), $Ba(NO_3)$ (Acros Organics, 99%), and $Cu(NO_3)_2$, 3 H_2O (Sigma Aldrich 99.1%) are dissolved in distilled water (250 ml), with a respective molar ratio of 1:2:3 in cations (in order to obtain the convenient stoichiometry $YBa_2Cu_3O_{7-\delta}$ after a heat treatment) and a total concentration in cations of 1.2 M. Organic compounds (HMTA and acac) are dissolved into acetic acid with a molar ratio of 1:1. The nitrates and the organic compounds are then mixed with a ratio of 1:3.5 according to previous works [17] and the total volume is adjusted to 400 ml with acetic acid. The kinetics of the polymerization is increased by heating the mixture to 100 °C, until the total volume reaches 150 ml. A first step of calcination is carried out at 450 °C during 2 h with a heating rate of 100 °C/h according to previous work [18] in order to eliminate organic compounds then followed by a second treatment at 850 °C during 1 h with a heating rate of 100 °C/h under air flow in order to obtain crystallized $YBa_2Cu_3O_{7-\delta}$ without secondary phase as the green phase Y_2BaCuO_5. The black powder obtained is grounded in an agate ball mill at 400 rpm during 2 h in order to break the aggregates. The powder is used to prepare pellets (powder is melt with a binder and pressed in a pelletizer with a pressure of 15 t) in order to analyze their optical properties. 4 pellets are shaped and heat treated at 850 °C, 875 °C, 900 °C and 925 °C, under air flow, during 1 h, at a heating rate of 100 °C/h. The $YBa_2Cu_3O_{7-\delta}$ powder is also used to process suspensions in order to coat SiC pellets and analyze their optical properties too.

2.2. Processing of coatings on SiC pellets

$YBa_2Cu_3O_{7-\delta}$ thick films are prepared by dipping SiC pellets into the suspension. The $YBa_2Cu_3O_{7-\delta}$ powder is first dispersed in MEK–EtOH (60–40) azeotropic mixtures by using a commercial dispersant (Polyvinylpyrrolidone 3500 PVP K12, Acros Organics). In order to obtain a homogeneous suspension, 2.5% in weight of dispersant compared to $YBa_2Cu_3O_{7-\delta}$ powder is first dispersed in the azeotropic mixture and then powder (30% in weight) is added under constant magnetic stirring.

A withdrawal speed of 200 mm/min is used to prepare the films. After the dip-coating process, the $YBa_2Cu_3O_{7-\delta}$ film is dried at 90 °C and is finally heated to the convenient temperature (850 °C) under air flow by using a ramp of 100 °C/h, kept at this temperature for 1 h and then cooled to 500 °C during 10 h and finally allowed to cool to ambient temperature.

2.3. Characterization techniques

Powder structure is determined by X-ray diffraction using a BRUKER AXS D4 Endeavor diffractometer operating with a Cu-Kα radiation source.

$YBa_2Cu_3O_{7-\delta}$ pellets and coating microstructures are determined using a scanning electron microscope JEOL 6700F.

Optical properties of SiC and coated SiC are characterized with a BRUKER VERTEX 80v spectrometer in the spectral range of 500–25,000 cm^{-1} corresponding to the far, mid and near infrared ranges (FIR, MIR and NIR respectively) and the visible range. Measurements of diffuse reflection are realized with two integrating spheres, respectively a gold-coated sphere ($\varnothing = 75$ mm) associated with a liquid N_2 cooled HgCdTe detector to cover the range of 500–8500 cm^{-1} and a PTFE sphere ($\varnothing = 75$ mm) associated with a Silicon Diode detector to cover the range of 8500–25,000 cm^{-1}. Reference measurements are performed on caps respectively coated with gold and PTFE. Acquisitions are all made at room temperature under normal atmosphere.

3. Results and discussion

3.1. Synthesis of $YBa_2Cu_3O_{7-\delta}$

The black powder obtained after the heat treatment at 850 °C under air flow is analyzed by X-ray diffraction (Fig. 1). The powder is crystallized and the XRD pattern is indexed into the orthorhombic structure and a Pmmm space group (JCPDS n°00-050-1886). The $YBa_2Cu_3O_{7-\delta}$ powder obtained is pure according to these results. This powder is then used after gridding to realize pellets.

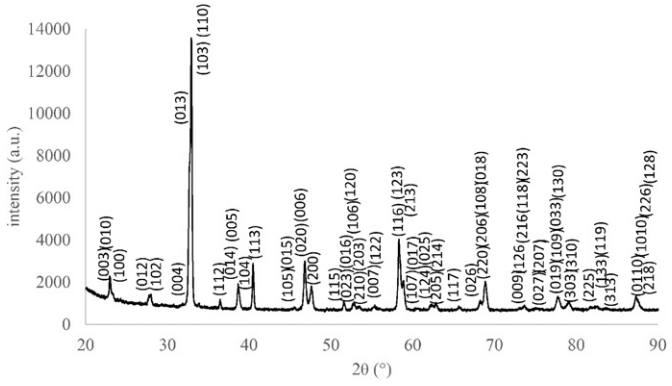

Fig. 1. XRD pattern of the $YBa_2Cu_3O_{7-\delta}$ powder obtained after a heat treatment at 850 °C under air flow.

3.2. $YBa_2Cu_3O_{7-\delta}$ pellets characterization

3.2.1. Pellet microstructure and oxygen stoichiometry

In order to obtain various oxygen stoichiometries (acting on 7-δ), 4 $YBa_2Cu_3O_{7-\delta}$ pellets are prepared and heat treated at 850 °C, 875 °C, 900 °C and 925 °C under air flow. Fig. 2 presents the different micrographs of the 4 pellets obtained after the heat treatments. We can observe that the higher the heat treatment is, the bigger the $YBa_2Cu_3O_{7-\delta}$ grains are. Indeed, grain size is multiplied by 3 when the heat treatment is 925 °C instead of 850 °C.

These results show the influence of the heat treatment on $YBa_2Cu_3O_{7-\delta}$ pellet microstructure, which can influence the spectral selectivity that we will see later. A complementary analysis by X-ray diffraction (Fig. 3) reveals differences between the 4 XRD patterns of the pellets. Indeed the peak indexed (200) at $2\theta = 46.7°$ is split into two other peaks indexed (200) and (020) when the heat treatment used is 850 °C or 925 °C respectively.

The structure of $YBa_2Cu_3O_{7-\delta}$ is tetragonal after an 850 °C heat treatment ($a = b \neq c$) and changes progressively into an orthorhombic structure when the heat treatment is increased ($a \neq b \neq c$). This change of structure (tetragonal to orthorhombic) is linked to the oxygen stoichiometry and the limit is around $\delta = 0.7$. This parameter can also act on spectral selectivity [13]; that is why we are trying here to evidence this parameter. We decided in this work to use a method developed by [16] based on crystallographic cell parameters: a, b and c parameters are related to oxygen stoichiometry and the orthorhombicity degree (evaluated by the formula $2(b - a)/(a + b)$). The a and b parameters are calculated by profile matching using the Fullprof software [19]. The oxygen stoichiometry is then estimated and all the results are gathered in Table 1: the δ coefficient decreases when the temperature increases. These results highlight that as the microstructure, the oxygen stoichiometry is directly linked to the heat treatment, which can influence the spectral selectivity.

3.2.2. Spectral selectivity in the IR-visible range

Spectral selectivity (and more particularly reflectance, knowing that in our case the transmittance is null on all the studied spectral range) is measured on the 4 $YBa_2Cu_3O_{7-\delta}$ pellets. The absorptance and the emittance are deduced from the reflectance values according to the Kirchhoff laws and the results are presented in Fig. 4.

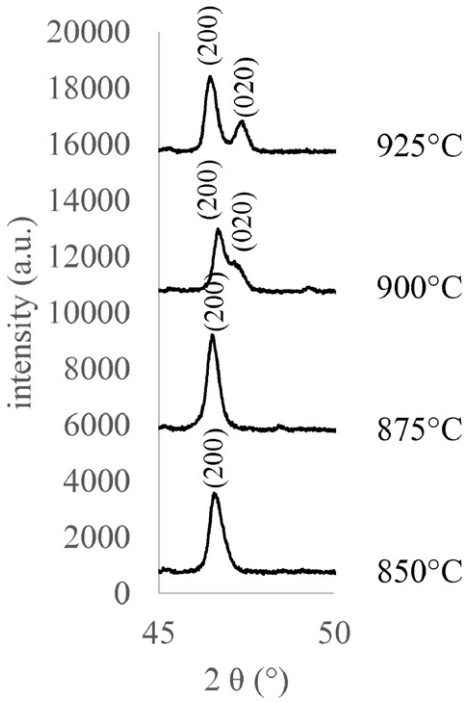

Fig. 3. XRD pattern between $2\theta = 45°$ and $2\theta = 50°$ of the YBCO pellets after different heat treatments.

The cutoff wavenumber of 5500 cm^{-1} had been defined by considering the thermal balance between the energy carried with concentrated solar rays with a factor of concentration of 1000 and the lost thermal energy imposed by the operating temperature of the receiver. This device must allow to raise the temperature of a fluid from 20 to 1000 °C when the fluid crosses through it. To quantify the efficiency of the $YBa_2Cu_3O_{7-\delta}$ pellets spectral selectivity the

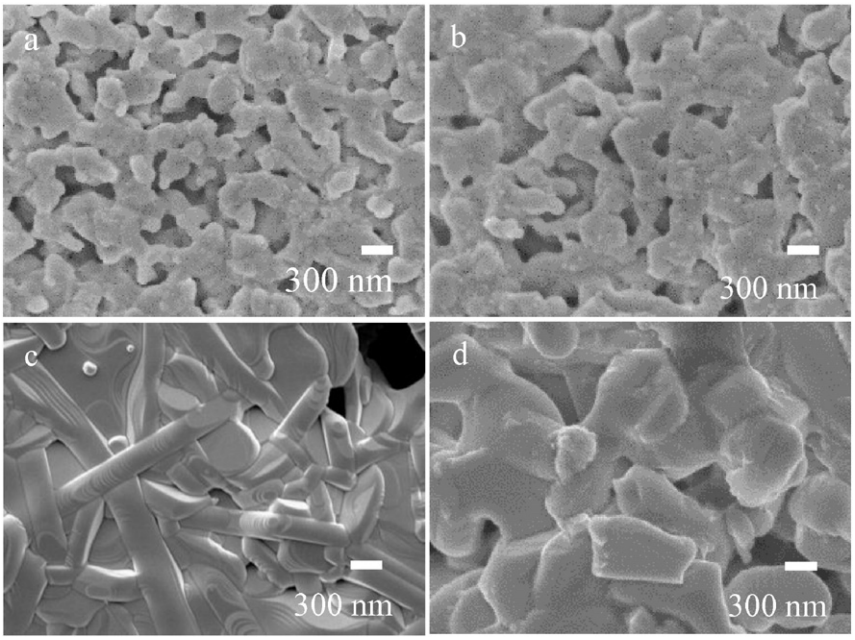

Fig. 2. Micrographs of the $YBa_2Cu_3O_{7-\delta}$ pellets after a heat treatment under air flow of a) 850 °C b) 875 °C c) 900 °C and d) 925 °C.

Table 1
estimation of the oxygen stoichiometry of the $YBa_2Cu_3O_{7-\delta}$ pellets depending on the heat treatment temperature.

	850 °C	875 °C	900 °C	925 °C
Crystallographic parameters (Å)	a = b = 3.855	a = b = 3.866	a = 3.846 b = 3.880	a = 3.825 b = 3.879
Orthorhombicity degree (%)	0 (tetragonal phase)	0 (tetragonal phase)	0.88	1.40
δ	>0.7	0.7	0.5	0.3

thermal emittance (ε_T) and the solar absorptance (α_S) are defined by the following equations:

$$\varepsilon_T(T) = \frac{\int_{\sigma_{min}}^{\sigma_{cutoff}} E(\sigma,T)B(\sigma,T)d\sigma}{\int_{\sigma_{min}}^{\sigma_{cutoff}} B(\sigma,T)d\sigma}$$

and

$$\alpha_S(T) = \frac{\int_{\sigma_{cutoff}}^{\sigma_{max}} E(\sigma,T)S(\sigma)d\sigma}{\int_{\sigma_{cutoff}}^{\sigma_{max}} S(\sigma)d\sigma}$$

where $S(\sigma)$ is the direct solar spectral irradiance [20] and $B(\sigma,T)$ is the well-known Planck's law [21] calculated at a given temperature T. The results are gathered in Table 2.

As expected [7], $YBa_2Cu_3O_{7-\delta}$ is highly absorbent in the NIR-visible range with solar absorptance values (α_S) of about 0.8–0.9 observed in the 4 cases. To compare, SiC pellet solar absorptance (α_S) is equal to 0.79 so the $YBa_2Cu_3O_{7-\delta}$ absorptance is better in the NIR-visible range. On the other hand, the thermal emittance values (ε_T) in the FIR-MIR range depend on the heat treatment used. Indeed, we can observe that the thermal emittance is lower when the thermal treatment is higher and a decrease of about 27% is reached when the pellet is heat treated at 925 °C.

These results mean that 2 parameters are involved and self-dependent: the pellet microstructure and the oxygen stoichiometry. According to Fig. 2 the microstructure is smoother when the sintering phenomenon is more important that is at higher temperature. The incident rays are more reflected and detected on smoother surfaces (as on $YBa_2Cu_3O_{7-\delta}$ pellets treated at 925 °C), on the contrary there are more reflection points on $YBa_2Cu_3O_{7-\delta}$ pellets treated at 850 °C leading the rays into the pellet attenuating the detected signal. These results are correlated with the $YBa_2Cu_3O_{7-\delta}$ pellets oxygen stoichiometry, indeed the best results are obtained for the highest oxygen stoichiometry ($\delta = 0.3$) reached at 925 °C. In order to obtain the highest reflectance

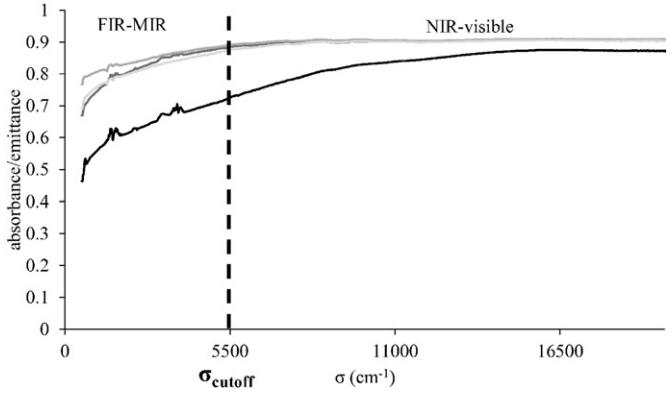

Fig. 4. Absorbance/emittance results of the $YBa_2Cu_3O_{7-\delta}$ pellets at room temperature in the MIR-NIR-visible range.

it is thus important to combine a smooth microstructure and a high oxygen stoichiometry.

3.3. $YBa_2Cu_3O_{7-\delta}$ coatings on SiC pellets

3.3.1. Implementation of an anti-diffusion layer

A first $YBa_2Cu_3O_{7-\delta}$ coating on SiC pellets is then realized by dip-coating. The pellet is immerge into the $YBa_2Cu_3O_{7-\delta}$ suspension described before. During the heat treatment, the $YBa_2Cu_3O_{7-\delta}$ coating reacted with the SiC substrate forming new phases as evidenced on the XRD pattern (Fig. 5-a). Indeed, barium is highly reactive at high temperature with carbon present in the SiC substrate forming thus a $BaCO_3$ phase. Many other phases are observed but are not indexed due to their quantity.

To avoid the diffusion phenomenon, an anti-diffusion layer has to be deposited. ZrO_2 is then chosen as the anti-diffusion layer because it has already proved its efficiency as a buffer barrier [22]. ZrO_2 is synthesized following the route derived from the Pechini's patent. As previously described two kinds of starting materials are used: inorganic compounds (in this case: zirconium oxynitrate $ZrO(NO_3)_2$, xH_2O (Acros Organics, 99.5%) with a cation concentration of 0.45 M) and organic compounds (acac and HMTA in an equimolar ratio and with a concentration of 0.70 M).

Once this sol is prepared, a first pre-coat is deposited in order to realize an anchorage film onto the substrate. A plasticizer is added in the sol (polyethyleneglycol PEG 35000, Aldrich, 60 g/L) according to optimized previous works [23]. This plasticizer allows the pre-coat to accommodate the constraints due to the surface roughness. After drying at 90 °C during 1 h pre-coated pellets are dipped again into the sol in which 1% in weight of commercial ZrO_2 (TOSOH-Zirconia TZ-0) is added. After removal of organic compounds and crystallization of the coating at 700 °C during 2 h (100 °C/h) the anti-diffusion layer is obtained, with a thickness of about 140 nm. The $YBa_2Cu_3O_{7-\delta}$ coating is then realized onto this layer, as described before but the 850 °C heat treatment is followed by an annealing at 500 °C during 10 h in order to control the oxygen stoichiometry [24]. During the heat treatment, the $YBa_2Cu_3O_{7-\delta}$ layer is preserved unlike the sample without the ZrO_2 anti-diffusion layer (as seen in Fig. 5-a and b).

3.3.2. Characterization of the coated SiC pellets

3.3.2.1. Coated pellet microstructure and oxygen stoichiometry. The surface of the $YBa_2Cu_3O_{7-\delta}$ coating is firstly analyzed by microscopy (Fig. 6-a) where a homogenous and covering coating can be observed. The cracks on the surface are due to the thermomechanical stresses appearing when coefficients of thermal expansion (CTE) are different between the substrate and the coatings. If we focus on the slice sample, SiC substrate and $YBa_2Cu_3O_{7-\delta}$ coating (about 10 μm thick) are easily identified

Table 2
Thermal emittance (ε_T) and solar absorptance (α_S) of a raw SiC pellet and $YBa_2Cu_3O_{7-\delta}$ pellets.

		$YBa_2Cu_3O_{7-\delta}$ pellets			
	SiC pellet	925 °C	900 °C	875 °C	850 °C
ε_T	0.89	0.65	0.83	0.85	0.82
α_S	0.79	0.84	0.90	0.91	0.90

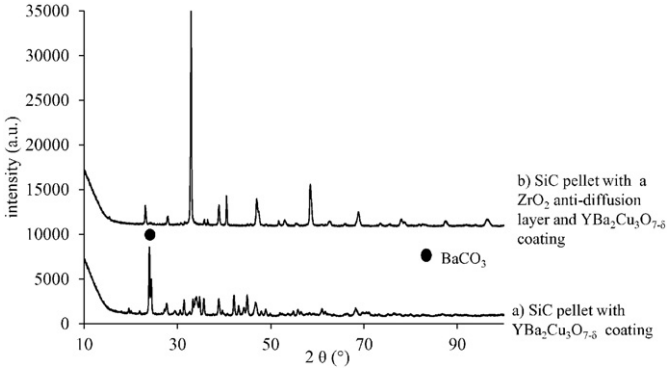

Fig. 5. XRD pattern of $YBa_2Cu_3O_{7-\delta}$ coating on SiC pellets with or without a ZrO_2 anti-diffusion layer.

(Fig. 6-b). An intermediate layer is also observed (about 2 μm thick), which seems denser than SiC and $YBa_2Cu_3O_{7-\delta}$. Indeed, the ZrO_2 anti-diffusion layer is a source of oxygen allowing the migration of silicon (from SiC) which reacts with the oxygen, the barium and the yttrium (from $YBa_2Cu_3O_{7-\delta}$) forming silicate oxides (as Ba_2SiO_4 or Y_2SiO_5). This intermediate layer composed of multiple oxides acts as a sacrificial barrier preventing the diffusion of $YBa_2Cu_3O_{7-\delta}$ into the SiC substrate.

The $YBa_2Cu_3O_{7-\delta}$ coating and an $YBa_2Cu_3O_{7-\delta}$ pellet heat treated at the same temperature (850 °C) present some microstructural differences (Fig. 6-c and d). First, the porosity is higher in the coating. Secondly, the grain sintering is less important in the coating. The conclusion is that the roughness is higher on the coating than on the pellet. As seen before, this high roughness influences the spectral selectivity of the $YBa_2Cu_3O_{7-\delta}$ coating.

The oxygen stoichiometry is determined by the profile matching of the XRD pattern which allows evidencing the crystallographic cell parameters and then using the method implemented by [16]. The cell parameters a and b are respectively equal to 3.856 Å and 3.883 Å and the orthorhombicity degree is then equal to 0.85%. The oxygen non-stoichiometry δ is close to 0.6 according to the Graf et al. works. The stoichiometry is higher when $YBa_2Cu_3O_{7-\delta}$ is used as a coating compared to the pellet heat treated at the same temperature. Indeed the oxygenation process is easier when the material is thinner.

3.3.2.2. Spectral selectivity in the IR-visible range. Reflectance is measured on a raw SiC pellet and on a coated SiC pellet with an anti-diffusion layer of ZrO_2 (about 140 nm thick) covered with an $YBa_2Cu_3O_{7-\delta}$ coating (about 10 μm thick). Absorptance and emittance results deduced from reflectance measurements are presented in Fig. 7. The SiC pellet presents a peak in the 790–1200 cm^{-1} range characteristic of the Reststrahlen band due to the SiC lattice vibrations [25]. Between 1200 cm^{-1} and 25,000 cm^{-1}, absorptance decreases until a minimum value of 0.78. When SiC is coated with $YBa_2Cu_3O_{7-\delta}$ the phonon peak observed at 825 cm^{-1} totally disappears meaning the coating is thicker enough and its spectral selectivity is predominant. This phenomenon is also existing in the NIR-visible range where we can observe the increase of the absorbance, compared to the raw SiC, until 0.97. The thermal emittance (ε_T) and the solar absorptance (α_S) are calculated to estimate the efficiency of the $YBa_2Cu_3O_{7-\delta}$ coating compared to the raw SiC pellet. These results are very promising, the $YBa_2Cu_3O_{7-\delta}$ coating is more absorbent ($\alpha_{SYBCO} = 0.93 > \alpha_{SSiC} = 0.79$ meaning an increase of about 18%) in the NIR-visible range than the raw SiC pellet knowing that it is of a great interest to increase the solar receiver absorptance. Moreover, the optical properties are predominant in the FIR-MIR range. However the emittance value is not as low as expected in the FIR-MIR range. Considering the non-stoichiometry δ of 0.6, a thermal emittance close to 0.8 was expected. As seen before, the roughness of the coating is higher than the $YBa_2Cu_3O_{7-\delta}$ pellet heat treated at the temperature. The conclusion is these results confirm that the coating microstructure is very important to reach a low emittance in the FIR-MIR range. The non-stoichiometry is controlled by a suitable heat treatment and can be increased, the next step will be the improvement of the microstructure of the $YBa_2Cu_3O_{7-\delta}$ coating by decreasing its roughness.

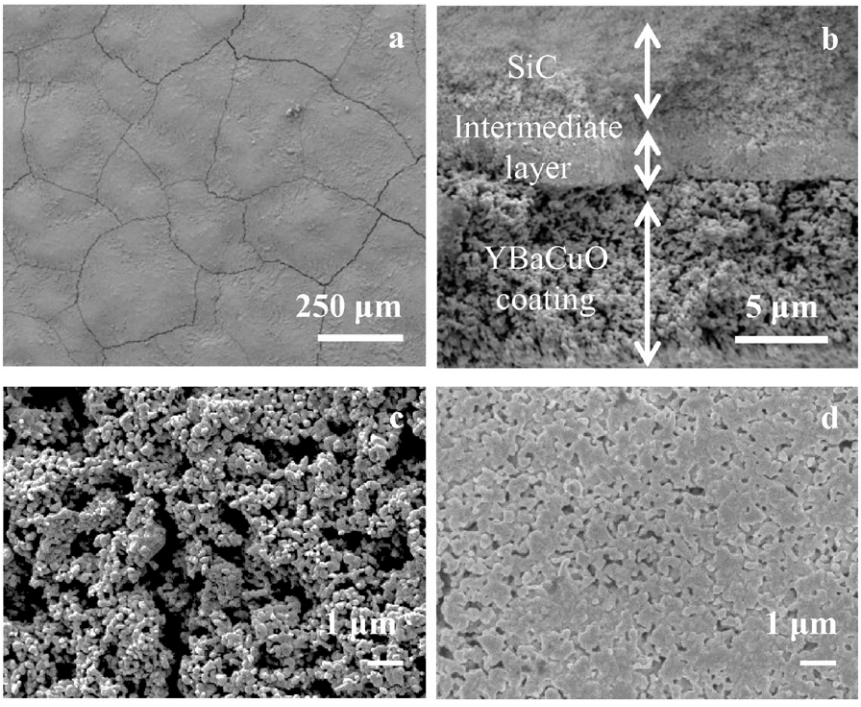

Fig. 6. Micrographs of $YBa_2Cu_3O_{7-\delta}$ coating treated at 850 °C followed by an annealing at 500 °C during 10 h a) surface general view b) slice view c) and d) comparison between $YBa_2Cu_3O_{7-\delta}$ coating and a $YBa_2Cu_3O_{7-\delta}$ pellet respectively, after this same heat treatment.

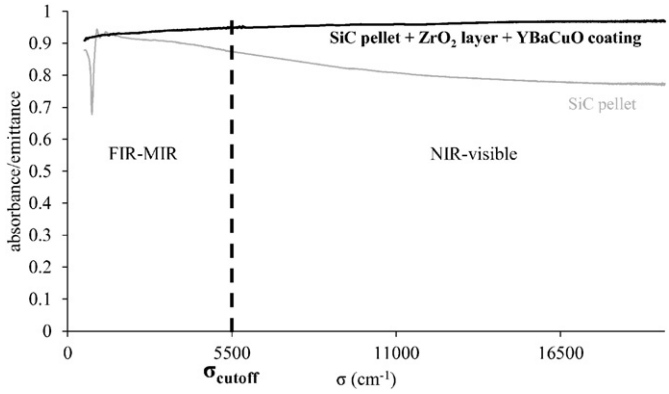

Fig. 7. influence of the $YBa_2Cu_3O_{7-\delta}$ coating on the SiC pellets absorbance/emittance.

4. Conclusion

In this study, we started the understanding of phenomena using a SiC planar substrate as reference exhibiting a non-optimized selectivity when used as solar receiver (this material absorbs all rays in the whole infrared-visible spectral domain). The aim was to realize an oxide layer with a better selectivity (reflecting in the FIR-MIR range and absorbing in the NIR-visible range). For this purpose, the $YBa_2Cu_3O_{7-\delta}$ oxide was chosen because of its specific optical properties. It was synthesized following a sol–gel route and it was obtained with a high level of purity. A first analysis on 4 various $YBa_2Cu_3O_{7-\delta}$ pellets reveals that the temperature of the heat treatment acts on both microstructure and oxygen stoichiometry. These two parameters lead to differences on the reflectance ability of the oxide. Indeed, to obtain the highest reflectance (and thus the lowest emittance) in FIR-MIR range, $YBa_2Cu_3O_{7-\delta}$ microstructure has to be the smoothest and $YBa_2Cu_3O_{7-\delta}$ oxygen stoichiometry has to be the highest. Considering these results, an $YBa_2Cu_3O_{7-\delta}$ coating was carried out onto SiC pellets, using a ZrO_2 anti-diffusion layer. Spectral selectivity of the coated pellet was very promising: it was predominant in the FIR-MIR range whereas absorptance was increased by about 18% in NIR-visible range. The next step will be the increase of the $YBa_2Cu_3O_{7-\delta}$ oxygen stoichiometry associated with a decrease of the coating roughness to reach the highest reflectance in the FIR-MIR range.

Acknowledgment

The French National Research Agency (ANR-11-SEED-00009) is gratefully acknowledged for its financial support in the framework of "Optisol" national project.

References

[1] T. Fend, R. Pitz-Paal, O. Reutter, J. Bauer, B. Hoffschmidt, Two novel high-porosity materials as volumetric receivers for concentrated solar radiation, Sol. Energy Mater. Sol. Cells 84 (2004) 291–304.
[2] B. Rousseau, S. Guevelou, G. Domingues, J. Vicente, C. Caliot, G. Flamant, Prediction of the Radiative Properties of Reconstructed Alpha-SiC Foams Used for Concentrated Solar Applications, MRS Online Proc. Libr., MRS Online Proceedings Library, 2013 1545.
[3] T. Menigault, G. Flamant, B. Rivoire, Advanced high-temperature two-slab selective volumetric receiver, Sol. Energy Mater 24 (1991) 192–203.
[4] A. Hall, A. Ambrosini, C. Ho, Solar selective coatings for concentrating solar power central receivers, Adv. Mater. Process. 170 (2012) 28–32.
[5] R. Bayón, G. San Vicente, C. Maffiotte, Á. Morales, Preparation of selective absorbers based on CuMn spinels by dip-coating method, Renew. Energy 33 (2008) 348–353.
[6] J. Vince, A. Šurca Vuk, U.O. Krašovec, B. Orel, M. Köhl, M. Heck, Solar absorber coatings based on CoCuMnOx spinels prepared via the sol–gel process: structural and optical properties, Sol. Energy Mater. Sol. Cells 79 (2003) 313–330.
[7] R. Lobo, C. Allançon, F. Gotor, J.-M. Bassat, L. Jean-Pierre, P. Odier, et al., Analysis of infrared-visible-near-ultraviolet reflectivity of conducting and superconducting oxides, Phys. C Supercond. 235-240 (1994) 1071–1072.
[8] B. Rousseau, A. Canizares, E. Véron, R. Ramy-Ratiarison, A. Blin, D. De Sousa Meneses, et al., Characterisation of $YBa_2Cu_3O_{6+x}$ films grown by the trifluoro-acetate metal organic decomposition route by infrared spectroscopy, Thin Solid Films 515 (2006) 1607–1611.
[9] P. Vermeir, J. Feys, J. Schaubroeck, K. Verbeken, P. Lommens, I. Van Driessche, Influence of sintering conditions in the preparation of acetate-based fluorine-free CSD YBCO films using a direct sintering method, Mater. Res. Bull. 47 (2012) 4376–4382.
[10] Y. Masuda, T. Tateishi, K. Matsubara, R. Ogawa, Y. Kawate, Preparation of $YBa_2Cu_3O_{7-x}$ (YBCO) superconductive film using sol–gel method, Jpn. J. Appl. Phys. 30 (1990) 1390–1397.
[11] V.F. Solovyov, H.J. Wiesmann, Q. Li, D.O. Welch, Three- and four- μm-thick $YBa_2Cu_3O_7$ layers with high critical-current densities on flexible metallic substrates by the BaF 2 process, J. Appl. Phys. 99 (2006) 1–6.
[12] M. Pechini, Method of Preparing Lead and Alkaline Earth Titanates and Niobates and Coating Method Using the Same to Form a Capacitor, 3,330,697, 1963.
[13] S. Sugai, Effects of oxygen deficiency on the infrared spectra in $YBa_2Cu_3O_{7-d}$, Phys. Rev. B 36 (1937) 7133–7136.
[14] M. Kakihana, L. Börjesson, S. Eriksson, P. Svedlindh, Fabrication and characterization of highly pure and homogeneous $YBa_2Cu_3O_7$ superconductors from sol–gel derived powders, J. Appl. Phys. 69 (1991) 867.
[15] E. Saiz, M.F. Barba, P. Ortega, J.S. Moya, Oxygen content determination in the $YBa_2Cu_3O_{7-\delta}$ compound, Mater. Lett. 8 (1989) 238–240.
[16] T. Graf, G. Triscone, J. Muller, Variation of the superconducting and crystallographic properties and their relation to oxygen stoichiometry of highly homogeneous $YBa_2Cu_3O_{7-\delta}$, J. Less-Common Met. 159 (1990) 349–361.
[17] P. Lenormand, S. Castillo, J.-R. Gonzalez, C. Laberty-Robert, F. Ansart, Lanthanum ferromanganites thin films by sol–gel process. Influence of the organic/inorganic R ratio on the microstructural properties, Solid State Sci. 7 (2005) 159–163.
[18] M.-L. Fontaine, C. Laberty-Robert, A. Barnabé, F. Ansart, P. Tailhades, Synthesis of $La_{2-x}NiO_{4+\delta}$ oxides by polymeric route: non-stoichoimetry control, Ceram. Int. 30 (2004) 2087–2098.
[19] J. Rodriguez-Carvajal, Detailed Description of Input Files for Fullprof, 2001.
[20] NREL, reference solar spectral irradiance: air mass 1.5, http://rredc.nrel.gov/solar/spectra/am1.5/2005.
[21] R. Siegel, J.R. Howell, Thermal Radiation Heat Transfert, Fourth ed., 2001.
[22] E.V. Pechen, R. Schoenberger, B. Brunner, S. Ritzinger, K.F. Renk, M.V. Sidorov, et al., Epitaxial growth of $YBa_2Cu_3O_{7-\delta}$ films on oxidized silicon with yttria- and zirconia-based buffer layers, J. Appl. Phys. 74 (1993) 3614.
[23] J. Mollicone, F. Ansart, P. Lenormand, B. Duployer, C. Tenailleau, J. Vicente, Characterization and functionalization by sol–gel route of SiC foams, J. Eur. Ceram. Soc. 34 (2014) 3479–3487.
[24] N. El Khokh, R. Papiernik, L.G. Hubert-Pfalzgraf, F. Chaput, J.P. Boilot, Preparation of YBaCuO powder by sol–gel techniques using molecular precursors, J. Mater. Sci. Lett. 8 (1989) 762–764.
[25] M.F. Macmillan, R.P. Devaty, W.J. Choyke, Infrared reflectance of thick p-type porous SiC layers, J. Appl. Phys. 80 (1996) 2412–2419.